THE JOURNAL OF PHYSICAL CHEMISTRY A

Article

pubs.acs.org/JPCA

Ab Initio Potential Energy Curves for the Ground and Low-Lying Excited States of OH and OH^- and a Study of Rotational Fine Structure in Photodetachment

Saurabh Srivastava[†] and N. Sathyamurthy*[,†,‡]

[†]Department of Chemistry, Indian Institute of Technology Kanpur, Kanpur 208016, India

[‡]Indian Institute of Science Education and Research Mohali, Sector 81, SAS Nagar, Manauli PO 140306, India

S *Supporting Information*

ABSTRACT: Complete basis set extrapolated ab initio potential energy curves obtained from multireference configuration interaction (MRCI) level calculations for the ground state ($X^1\Sigma^+$) of OH^-, and the ground state ($X^2\Pi$) and the first excited state ($A^2\Sigma^+$) of OH are reported. The potential energy curves for the excited states $A^1\Pi$, $a^3\Pi$, and $b^3\Pi$ of OH^- have been computed using the V6Z basis set at the MRCI level. Λ-doubling parameters p and q were calculated for the ground and the first excited vibrational states of the ground electronic state of OH using second-order perturbation theory. Using the computed potential energy curves and the rovibrational spectra for photodetachment including the fine splitting, the threshold for electron detachment has been computed. The result is in agreement with the experimental results of Goldfarb et al. [*J. Chem. Phys.* **1985**, *83*, 4364].

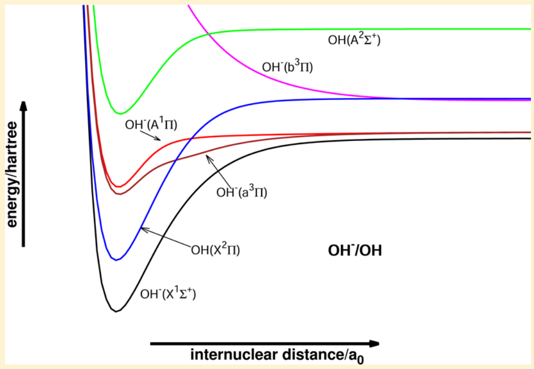

INTRODUCTION

As an important anion, OH^- has been studied extensively by experimentalists as well as theoretical groups. The first photoelectron spectrum of OH^- was recorded by Branscomb,[1] and an electron affinity value of 1.38 ± 0.04 eV was obtained for OH. Celotta et al.[2] used a fixed frequency ion laser to obtain the photodetachment spectra of some di- and triatomic anions including OH^- and obtained a threshold of $1.829^{+0.010}_{-0.014}$ eV for electron detachment from OH^-. Hotop et al.[3] obtained the photoelectron spectra for OH^- and OD^- in the range of 7000−6450 Å and reported the electron affinity of OH as 1.825 ± 0.002 eV. Saykally and coworkers[4,5] recorded the rovibrational spectra of OH^-. Goldfarb et al.[6] performed a photodetachment experiment to record the P, Q, and R branches of the $OH^-(\nu = 0)$ to OH ($\nu = 0$) detachment threshold and recommended an electron affinity value of 1.8276487(11) eV for OH. Wester and coworkers[7] determined the photodetachment cross section values for a cold OH^- using a lower depletion tomography method in a multipole radio frequency ion trap. Aravind et al.[8] used a crossed anion-laser interaction and a linear time-of-flight photoelectron spectrometer to measure the angular distribution of photoelectrons detached from OH^-. Recently Otto et al.[9] have shown that near-threshold photodetachment spectroscopy of trapped and buffer-gas-cooled OH^- is capable of measuring internal state populations.

To the best of our knowledge, the first theoretical study of the OH^- anion was by Cade[10] using Hartree−Fock−Roothaan matrix equations, and he predicted the electron affinity of OH to be equal to 1.91 eV. Rosmus and Meyer[11] obtained an electron affinity value of 1.51 eV using PNO−CI and CEPA wave functions. Sun and Freed[12] used a quasi-degenerate many-body perturbation theory to obtain the ground-state energy and the vertical excitation energy values for the first four lowest excited states of OH^-. Werner et al.[13] calculated the potential energy and dipole moment functions for the ground state of OH^+, OH, and OH^- from MCSCF, MCSCF-SCEP, and SCEP-CEPA electronic wave functions. They reported vibrational transition probabilities for the ground electronic state of these diatomic species and an electron affinity value of 1.59 eV for OH at the MC-SCEP level of theory. Chipman[14] studied the effect of different reference models and different basis functions with MCSCF and MCSCF-CI methods and obtained the best estimate for the electron affinity of OH as 1.51 eV. A Møller−Plesset perturbation theoretical study at second- (MP2), third- (MP3), and fourth-order (MP4) levels was carried out by Frenking and Koch[15] to calculate the electron affinity of diatomic hydrides, and the best value of 1.79 eV was obtained for OH. The effect of several basis sets on the value of electron affinity at the SCF level of theory was investigated by Lee et al.,[16] and they found that the use of polarization functions was more important than the use of diffuse functions for a proper description of anions. Another work using a fourth-order many body perturbation theory (MBPT(4)) was by Ortiz,[17] for

Special Issue: Franco Gianturco Festschrift

Received: October 7, 2013
Revised: January 9, 2014

 © XXXX American Chemical Society dx.doi.org/10.1021/jp409940m | *J. Phys. Chem. A* XXXX, XXX, XXX−XXX

several mono-, di-, and tri-atomic anions, and he obtained a value of 1.764 eV for the electron affinity of OH.

Pluta et al.[18] performed MBPT(4) calculations to determine the polarizability and electron affinity of OH. They obtained a value of 1.82 eV for the electron affinity. Tellinghuisen and Ewig[19] calculated potential energy curves (PECs) and spectroscopic constants for the ground and low-lying excited electronic states of OH and OH^- in vacuum and in an fcc lattice at the MCSCF level of theory. They proposed that the vibrationally bound $^1\Pi$ and $^3\Pi$ states of the anion are responsible for the UV luminescence spectrum of OH^- in alkali halides. These states are found to be 3 to 4 eV above the ground state of the anion. Indirect spin−spin coupling constant and its temperature dependence were studied by Sauer et al.[20] using the second-order polarization propagator approximation (SOPPA) with coupled cluster singles and doubles (CCSD) amplitudes. Another important theoretical work has been done by Ortiz[21] to calculate the electron detachment energy of closed-shell anions including OH^- with an ab initio implementation of the electron propagator approximation. He obtained a value of 1.853 eV for the electron affinity of OH.

In the present work, we report accurate PECs for the ground and a few excited states of OH^- and the ground and the first excited state of OH. We have calculated the photodetachment rovibrational spectra including *P*, *Q*, and *R* branches arising from Λ-doubling in OH. Consequently, a possible value for the threshold for electron detachment is also reported.

■ THEORETICAL METHODS

Spin−Orbit Coupling. The interaction between the spin and orbital angular momenta of the electrons is added as a perturbation to the electronic Hamiltonian, and the total Hamiltonian operator is written as:

$$H^{TOT} = H^0 + H^{SO} \tag{1}$$

where H^0 and H^{SO} are the unperturbed Hamiltonian and the spin−orbit coupling, respectively. The Breit−Pauli perturbation term (H^{SO}) is given as[22]

$$H^{SO} = \frac{\alpha^2}{2}\sum_i \left\{\frac{Z_A}{r_{iA}^3}\boldsymbol{l}_{iA}\cdot\boldsymbol{s}_i + \frac{Z_B}{r_{iB}^3}\boldsymbol{l}_{iB}\cdot\boldsymbol{s}_i\right\} - \frac{\alpha^2}{2}\sum_{i\neq j}\frac{1}{r_{ij}^3}(\boldsymbol{r}_{ij}\times\boldsymbol{p}_i)(\boldsymbol{s}_i + 2\boldsymbol{s}_j) \tag{2}$$

where the index *i* refers to the electrons and *A* and *B* refer to the two nuclei in a diatomic species *AB*. $\alpha = 1/137.036$ is the fine structure constant, and $\boldsymbol{l}$ and $\boldsymbol{s}$ are the orbital and spin angular momenta, respectively. $\boldsymbol{p}$ is the linear momentum of the electron. r_{iA} and r_{iB} are the distances between the *i*th electron and the nuclei *A* and *B*, respectively, while r_{ij} is the distance between electrons. The first part of eq 2 is defined as the direct spin−orbit interaction and is a single electron operator, while the second part is the spin-other orbit interaction and a two electron operator.

Because of the coupling of angular momenta, the total orbital angular momentum Λ and the total spin angular momentum Σ are no longer good quantum numbers. The good quantum number $\Omega = \Lambda+\Sigma$ and the states corresponding to Λ and Σ correlate with the components of Ω. The $X^2\Pi$ state of OH splits into $^2\Pi_{3/2}$ and $^2\Pi_{1/2}$ components. The selection rules[23] for the matrix elements of H^{SO} can be summarized as:

$$\Delta\Omega = 0;\ \Delta S = 0, \pm 1;\ \Delta\Lambda = -\Delta\Sigma = 0, \pm 1;\ \Sigma^+ \leftrightarrow \Sigma^- \tag{3}$$

It should be noted here that in the single-configuration limit, if the two interacting states belong to the same configuration, then $\Delta\Lambda = \Delta\Sigma = 0$. If the two states differ by at the most one spin−orbital, then $\Delta\Lambda = -\Delta\Sigma = \pm 1$.

This selection rule allows spin−orbit coupling between $X^2\Pi$, and $A^2\Sigma^+$ states of OH. The spin−orbit coupling constant (*A*) can be defined for the diagonal matrix elements of H^{SO} such that[22]

$$\langle \Lambda, \Sigma, \Omega, S, v|H^{SO}|\Lambda, \Sigma, \Omega, S, v\rangle = A_{\Lambda,v}\Lambda\Sigma \tag{4}$$

where *S* and *v* are spin angular momentum and vibrational quantum number, respectively. The calculation of off-diagonal matrix elements of H^{SO} and the spin−orbit coupling constant for the $X^2\Pi$ state of OH is discussed later in the text.

■ RESULTS AND DISCUSSION

Potential Energy Curves and Vibrational Bound States. Calculations of potential energy values for the ground-state $X^1\Sigma^+$ and three lowest excited states $A^1\Pi$ and $a,b^3\Pi$ of OH^- and the ground state $X^2\Pi$ and the excited state $A^2\Sigma^+$ of OH were carried out at the MRCI level of theory using the diffusely augmented aug-cc-pV*X*Z(AV*X*Z) basis and the segmented cc-pV*X*Z(V*X*Z) basis of Dunning and coworkers[24−26] for 72 values of the internuclear distance (*R*) of OH^- ranging from $0.8a_0$ to $15.0a_0$ using MOLPRO suite of programs.[27] State-averaged full-valence CASSCF calculations with four σ and two π orbitals were used to obtain the reference orbitals for the MRCI calculation. The molecular orbital configuration for the $X^1\Sigma^+$ state of OH^- is $\sigma_{1s}^2\sigma_{2s}^2\sigma_{2p}^2\pi_{2p}^4$, whereas $A^1\Pi$ and $a^3\Pi$ states have the same configuration of $\sigma_{1s}^2\sigma_{2s}^2\sigma_{2p}^2\pi_{2p}^3\sigma_{2p}^{*1}$ but different multiplicities. The potential energy values were extrapolated to the complete basis set (CBS) limit using the uniform singlet and triplet electron-pairs (USTE) method proposed by Varandas,[28,29] for the ground state of OH and OH^-. The potential energy values for the excited states of OH^- were not extrapolated and were computed at the MRCI/cc-pV6Z level of theory.

As was pointed out in our previous work, it is known[30−32] that the excited states of diatomic molecular anions are often embedded in the continuum of the neutral plus electron system, often described as Breit−Wigner resonances. The excited states of OH^- ion also show a similar behavior, as illustrated in Figure 1, and it can be observed that the excited states $A^1\Pi$ and $a^3\Pi$ are buried in the continuum of OH plus electron in the Franck−Condon region.

A careful examination of the dependence of the PECs of these two excited states on the basis set, shown in Figure 2, reveals that the use of a large augmented basis set results in the wrong limit. Therefore, second moment calculations[30−32] (see Supporting Information) were used to establish the correct PECs for the excited states ($A^1\Pi$ and $a^3\Pi$) of OH^- using the cc-pV6Z basis set. For the PECs for the ground state of OH and OH^-, a CBS extrapolation was done using the aug-cc-pV*X*Z (*X* = *T*, *Q*, 5, 6) basis sets for CAS energy and aug-cc-pV*X*Z (*X* = 5, 6) basis sets for the dynamic correlation energy. The resulting PECs for the ground and the excited states of OH and OH^- are plotted in Figure 1. Vibrational bound-state calculations have been performed using the ab initio PECs and the Fortran code LEVEL 8.0[33] of LeRoy. The resulting

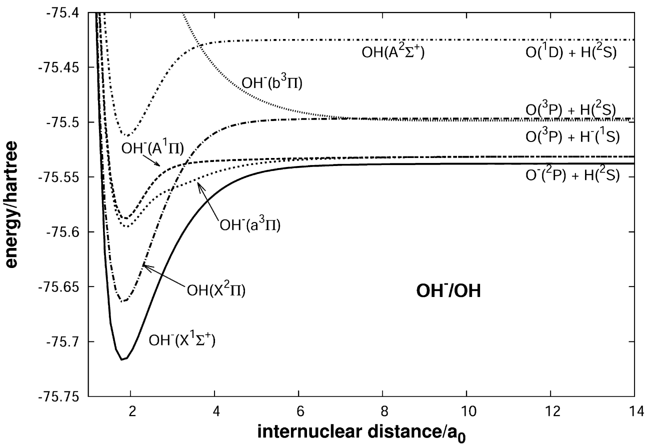

Figure 1. Potential energy curves for the ground state of OH^- and the ground state of OH obtained at the MRCI/CBS level of theory. The excited states of OH^- and OH are calculated at the MRCI level of theory using the V6Z basis set. The asymptotic energy value for the $X^1\Sigma^+$ state of OH^- is −75.53760749. The asymptotic energy values for the $A^1\Pi$, $a^3\Pi$, and $b^3\Pi$ states of OH^- are −75.53131167, −75.53131167, and −75.49801467, respectively. The asymptotic energy values for OH ($X^2\Pi$) and OH ($A^2\Sigma^+$) are −75.49665623 and −75.42479652 hartree, respectively.

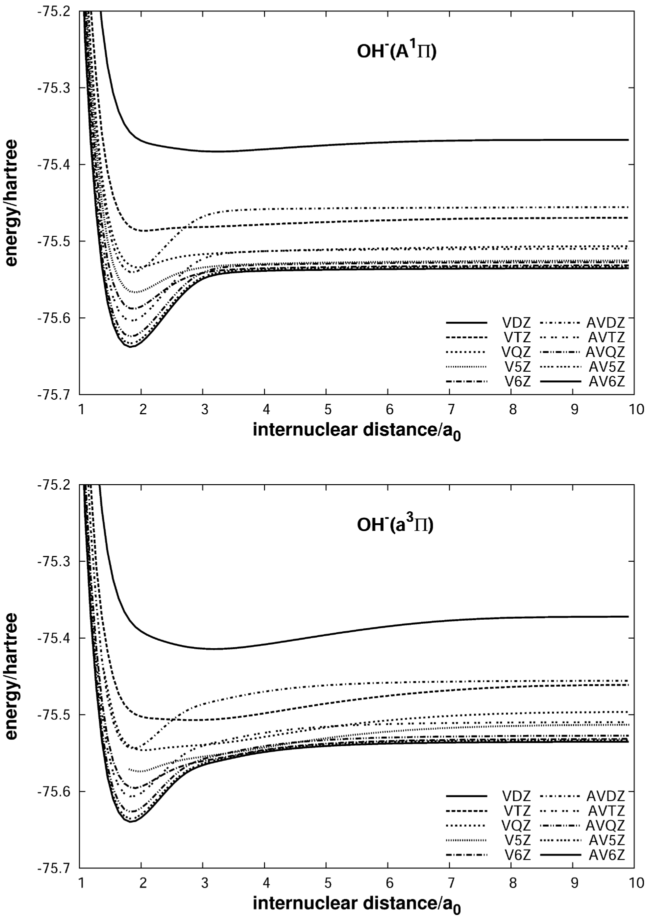

Figure 2. Potential energy curves for $A^1\Pi$ and $a^3\Pi$ states of OH^- obtained at the MRCI level of theory using AVXZ and VXZ ($X = D$, T, Q, 5, 6) basis sets.

spectroscopic constants are reported and compared with the previous reported values in Table 1.

Fine Structure and Λ Doubling. It is known that the ground state ($X^2\Pi$) of OH interacts with the excited state ($A^2\Sigma^+$) such that the rotational perturbation or Λ-doubling occurs in the ground state. As a result, the rotational levels in the ground electronic state split into two levels with different parities. The calculation of the Λ-doubling requires the spin−orbit coupling constant for the ground state of OH. The z component of the spin−orbit coupling operator ($a_i l_{zi} s_{zi}$) has all of the diagonal elements. Akin to NH^-, the configuration $\sigma^2\pi^3$ results in values for the matrix elements $\langle ^2\Pi_{1/2}|H^{SO}|^2\Pi_{1/2}\rangle = -A_e$ and $\langle ^2\Pi_{3/2}|H^{SO}|^2\Pi_{3/2}\rangle = +A_e$. It is, therefore, an inverted state as opposed to the π^1 configuration. We have used MOLPRO[27] to calculate the spin−orbit coupling constant (A_e) for these diagonal elements for different values of R in the range $0.8a_0 - 10.0a_0$. The results are plotted in Figure 3.

The upper curve in Figure 3 was obtained when the calculations were done with the $X^2\Pi$ state only, and the lower curve was obtained when the $A^2\Sigma^+$ state was included in the spin−orbit calculation. The calculations were done by using the state-interacting method[34] implemented in MOLPRO. It can be seen that the inclusion of the $A^2\Sigma^+$ state increases the magnitude of the spin−orbit coupling constant by nearly 10 cm^{-1} for all geometries. The inclusion of the $A^2\Sigma^+$ state gives a Coriolis term (off-diagonal spin−orbit coupling term), which cannot be neglected in the calculation of the spin−orbit coupling, as pointed out by Parlant and Yarkony[35] that the contribution of $H(^2S)$ to the electronic angular momentum relative to the center of mass of OH is significant. The spin−orbit coupling constant (A_v) for a given vibrational level is calculated as

$$A_v = \int_R |\chi_v(R)|^2 A_e(R) \tag{5}$$

where $\chi_v(R)$ is the wave function for the vibrational state v and the A_e values are taken from the lower curve of Figure 3. The computed A_v values are in good agreement with the experimental values reported by van der Loo and Groenenboom[36] and with the theoretical results of Coxon and Foster[37] with an error of <1 cm^{-1}. The asymptotic value of A_e is nearly 100 cm^{-1}, in agreement with the results of Langhoff et al.[38] having the correct asymptote of OH dissociating into $O(^3P)$ + $H(^2S)$. It should be pointed out that the vibrational wave functions are calculated with the nonrelativistic PECs, which could be a reason for the slight differences between our present results and previous works.

Mulliken and Christy[39] defined the terms p_v and q_v, known as Λ-doubling constants, arising from the interaction between all $^2\Sigma$ states and the $^2\Pi$ state. These terms are given by

$$p_v^{\Pi}(^2\Sigma^s) = 2\sum_{^2\Sigma,v'} (-1)^s \langle ^2\Pi, v|\sum_i a_i l_i^+ s_i^- |^2\Sigma^s, v'\rangle \times \frac{\langle ^2\Sigma^s, v'|\frac{\hbar^2}{2\mu R^2}\sum_i l_i^- |^2\Pi, v\rangle}{E_{\Pi,v} - E_{\Sigma,v'}} \tag{6}$$

$$q_v^{\Pi}(^2\Sigma^s) = 2\sum_{^2\Sigma,v'} \frac{|\langle ^2\Pi, v\left|\frac{\hbar^2}{2\mu R^2}\sum_i l_i^+\right|^2\Sigma^s, v'\rangle|^2}{E_{\Pi,v} - E_{\Sigma,v'}} \tag{7}$$

where the summation goes over all vibrational levels of all relevant excited $^2\Sigma^{\pm}$ electronic states. The exponent s is zero for $^2\Sigma^+$ states and 1 for $^2\Sigma^-$ states. The operators l_i^+ and s_i^- are the raising and lowering operators for the orbital angular

dx.doi.org/10.1021/jp409940m | J. Phys. Chem. A XXXX, XXX, XXX−XXX

Table 1. Spectroscopic Constants for the Ground and Excited States of OH and OH^- [a]

species	state	method[ref.]	energy (a.u.)	R_e (Å)	ω_e (cm^{-1})	$\omega_e x_e$ (cm^{-1})	B_e (cm^{-1})	α_e (cm^{-1})	D_e (cm^{-1})	T_e (cm^{-1})
OH^-	$X^1\Sigma^+$	MRCI/CBS	−75.732444	0.9685	3838	98.93	18.98	0.736	0.001872	0.0
		PNO-CEPA[11]	−75.69325	0.961	3809	94	19.23	0.766		0.0
		MCSCF-SCEP[13]	−75.70566	0.967	3731	92	19.02	0.791		0.0
		MCSCF[19]		0.9666	3759	97.9				0.0
		exp.[43]			3680 ± 37		19.13	0.773		0.0
	$A^1\Pi$	MRCI/V6Z	−75.588120	0.9905	3299	89.56	17.96	0.723	0.002218	31675
	$a^3\Pi$	MRCI/V6Z	−75.595654	1.0000	3057	86.94	17.50	0.745	0.002485	30022
OH	$X^2\Pi$	MRCI/CBS	−75.663761	0.9690	3719	85.83	18.94	0.758	0.001889	0.0
		exp.[44]		0.9697	3737.76	84.88				0.0
		MCSCF[19]		0.9745	3741	86.8				0.0
	$A^2\Sigma^+$	MRCI/CBS	−75.512726	1.0100	3230	101.57	17.40	0.770	0.002015	33148
		exp.[44]		1.0121	3178.86	92.92				32684
		MCSCF[19]		1.0214	3124	101				33912

[a]Calculated by fitting the vibrational and rotational states to the equation $E_{v,J} = (v + 1/2)\omega_e - (v + 1/2)^2\omega_e x_e + B_e J(J + 1) - \alpha_e(v + 1/2)J(J + 1) - D_e[J(J + 1)]^2$

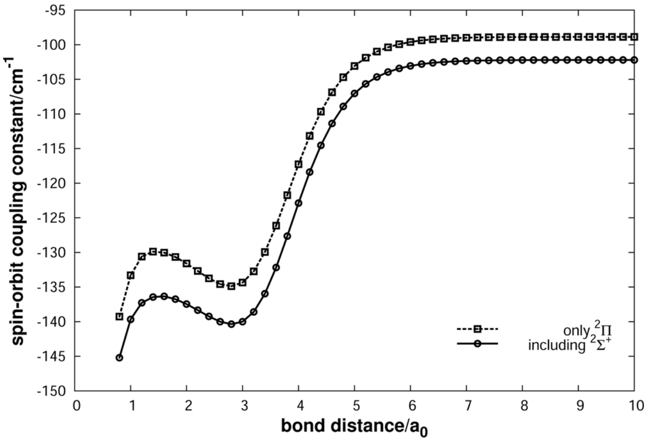

Figure 3. Values of the spin−orbit coupling constant for the ground electronic state ($X^2\Pi$) of OH obtained at the MRCI level of theory using the AV6Z basis set.

momentum and the spin angular momentum, respectively, for the ith electron. The operator a_i contains the radial part of the Breit−Pauli Hamiltonian. The off-diagonal elements of the spin−orbit matrix for a diatomic hydride can be calculated in terms of the spin−orbit coupling constant of the diagonal elements using a *pure precession approximation*. This approximation requires that each of the interacting $^2\Pi$ and $^2\Sigma$ states is well-described by a single configuration and that the two states differ by a single spin−orbital. In addition, the spin−orbital is a pure atomic orbital such that[22]

$$\mathbf{l}^{\pm}|nl\lambda\rangle = [l(l + 1) - \lambda(\lambda \pm 1)]^{1/2}|nl\lambda \pm 1\rangle \quad (8)$$

where n, l, and λ are quantum numbers for an atomic orbital. The approximation takes the *simple pure precession* form for the $X^2\Pi - A^2\Sigma^+$ interaction because the valence orbital configurations corresponding to these two states can be written as π^1 and σ^1, respectively, as the other orbitals are completely filled and they make zero contribution to the total angular momentum. Therefore, the Λ-doubling parameters for the $X^2\Pi - A^2\Sigma^+$ interaction become

$$p_v(^2\Sigma^+) = 4A_v B_v/\Delta E_{\Pi\Sigma} \quad (9)$$

$$q_v(^2\Sigma^+) = 4B_v^2/\Delta E_{\Pi\Sigma} \quad (10)$$

The computed values of the spin−orbit coupling constant and the Λ-doubling parameters are listed in Table 2. The values of the Λ-doubling parameters obtained are in accord with the results of Mulliken and Christy[39] but not with other experimental or theoretical values reported. The reason as shown by Hinkley et al.[40] may be the inclusion of only the ground vibrational state of OH in the calculation of these parameters by Mulliken and Christy and by us. Furthermore, other calculations involve RKR potentials, which show a larger well depth than the MRCI/CBS results obtained in the present study, but this difference in the values of p_v and q_v does not affect the Λ-doubling results, and an error of only 0.03% was found.

Experiments[3,6] suggest that photodetachment near threshold occurs via the following sequence of reactions:

Table 2. Spin-Orbit Coupling Constant and Λ-Doubling Parameters for the Ground and the First Excited Vibrational State of OH in Its Ground Electronic State

v	A_v	ref.	v	p_v^Π	q_v^Π	ref.
0	−140.1397	present work[a]	0	0.296	−0.0418	present work
1	−139.8667	present work[a]	1	0.289	−0.0393	present work
0	−139.2729	van der Loo et al.[36]	0	0.235	−0.0386	Coxon and Foster[37]
1	−139.5410	van der Loo et al.[36]	1	0.224	−0.0369	Coxon and Foster[37]
0	−139.054	Coxon and Foster[37]	0	0.242	−0.0391	Hinkley et al.[40]
1	−139.325	Coxon and Foster[37]	0	0.311	−0.0417	Mulliken and Christy[39]
			0	0.246	−0.0384	Moore and Richards (Exp.)[45]

[a]Calculated at the MRCI/CBS level of theory using the states $X^2\Pi$ and $A^2\Sigma^+$.

Table 3. Photodetachment Rotational Fine Structure of OH^-

	$\Omega = 1/2$						$\Omega = 3/2$					
	theory[a]			experiment[6]			theory[a]			experiment[6]		
J''	P	Q	R	P	Q	R	P	Q	R	P	Q	R
0			15104.618			14867.432			14977.538			14740.982
1		15067.625	15128.647			14891.272		14940.248	15024.475			
2	14992.986	15054.642	15155.753		14816.134		14865.906	14949.839	15069.040	14628.645	14712.566	
3	14942.746	15044.725	15185.329		14805.211		14838.574	14957.032	15111.944		14718.828	
4	14895.808	15037.296	15216.887		14796.347		14809.095	14962.584	15153.798		14722.978	14910.666
5	14851.656	15031.916	15250.126		14788.899		14778.271	14967.158	15195.125		14725.532	
6	14809.893	15028.334	15284.923		14782.400		14746.804	14971.329	15236.392			
7	14770.305	15026.476	15321.300		14776.505		14715.304	14975.612	15278.039			
8	14732.856	15026.413	15359.394				14684.325	14980.494	15320.498			
9	14697.655	15028.330	15399.439				14654.394	14986.453	15364.213			

[a] Present work.

Table 4. Electron Affinity of OH

electron affinity (eV)	method[reference]	electron affinity (eV)	method[reference]
1.83 ± 0.04	exp.[1]	1.51	MCSCF-CI[14]
$1.829^{+0.010}_{-0.014}$	exp.[2]	1.764	MBPT(4)[17]
1.825 ± 0.002	exp.[3]	1.79	MP4[15]
1.82765	exp[6]	1.76	EOM[46]
1.91	Hartree–Fock[10]	2.07	variation-perturbation[47]
1.51	CEPA[11]	1.82	MBPT(4)[18]
1.59	MC-SCEP[13]	1.857	present work

$$OH^-(^1\Sigma^+; J'') + h\nu \rightarrow (OH + e^-)(^1\Pi; J_C) \quad (11)$$

$$(OH + e^-)(^1\Pi; J_C) \rightarrow OH(^2\Pi_{1/2,3/2}; J') + e^- \quad (12)$$

where J'' is the angular momentum of the negative ion and J' is the angular momentum of the final state of neutral OH. J_C represents the total angular momentum of the $^1\Pi$ state of the neutral plus electron complex. For the transition from the ground rotational state to the excited rotational state, a change of parity is required by the dipole selection rule, and the conservation of angular momentum requires that $J_C = J''$ or $J'' \pm 1$. According to Hotop et al.[3] and Blondel et al.,[41] photodetachment microscopy works only for very low values of the initial kinetic energy of the departing electron, and the electron comes out practically as a pure *s* wave. Thus, the electron leaves with only the spin angular momentum 1/2. Therefore, the allowed final transitions are such that $J' = J'' \pm 1/2$ and $J' = J'' \pm 3/2$. Because OH also follows Hund's case (b), the nuclear rotational quantum numbers N' and N'' for OH and OH^-, respectively, are equal to the total angular momentum excluding the spin angular momentum of the electron. Therefore, we can write $N' = J' - 1/2$ for $\Omega = 1/2$ and $J' = J + 1/2$ for $\Omega = 3/2$ for the ground state of OH and $N'' = J''$ for the ground state of OH^-.

To obtain the rotational structure of photodetachment spectrum, we calculated the energy difference between the rotational fine structure of the ground state of OH^- and Λ-doubling states of the ground state of OH. The *P*, *Q*, and *R* branches for the photodetachment transition can be defined in terms of the transitions from the N'' state of OH^- to the $N' = N'' - 1$, N'', and $N'' + 1$ states, respectively. The values for the *P*, *Q*, and *R* branches for each of the Ω value of the ground state $X^2\Pi$ of OH are given in Table 3 along with the experimental values of Goldfarb et al.[6] It can be inferred from Table 3 that our theoretical values are in good agreement with the experimental values.

■ ELECTRON AFFINITY OF OH

The photodetachment spectrum of OH^- places a lower limit on the electron affinity of OH. The transition from the ground rovibrational state ($\nu = 0$, $J'' = 0$) of OH^- to the ground rovibrational state of OH ($\nu = 0$, $J' = 3/2, \Omega = 3/2$) is the lowest energy transition from the ground electronic state of OH^-, and it has a value of 14 977.538 cm^{-1} (1.857 eV). The value of the electron affinity obtained is in good agreement with the experimentally reported value of 14 740.982 cm^{-1} (1.827 eV). A comparison of our computed electron affinity value with different theoretical and experimental values is given in Table 4.

According to eq 11, electron detachment occurs via an electron-neutral complex of the $^1\Pi$ state of OH^-. We have calculated the energy gap between the ground vibrational state of the ground electronic state ($X^1\Sigma^+$) of OH^- and the ground vibrational state of the $A^1\Pi$ electronic excited state of OH^- to be 26 626 cm^{-1}(3.3 eV).

■ COMPARISON WITH NH^-

The PECs for the ground state ($X^2\Pi$) and the two low-lying excited states ($A^2\Sigma^+$, $B^2\Sigma^-$) of OH are compared with those for the ground state ($X^2\Pi$) and the excited states ($A^2\Sigma^+$, $A'^2\Sigma^-$) of the isoelectronic species[32] NH^- in Figure 4. It was expected that the ordering of electronic states would be the same for both the isoelectronic species. Although the PEC for the ground state of OH is comparable to that of NH^-, there is a noticeable discrepancy between the first two excited states of the two systems. The PEC for the $A^2\Sigma^+$ state of OH is qualitatively similar to that of NH^-, but there is a lower lying $A'^2\Sigma^-$ curve for NH^- and not for OH. The asymptotically lower energy curve $B^2\Sigma^-$ of OH crosses the $A^2\Sigma^+$ curve around

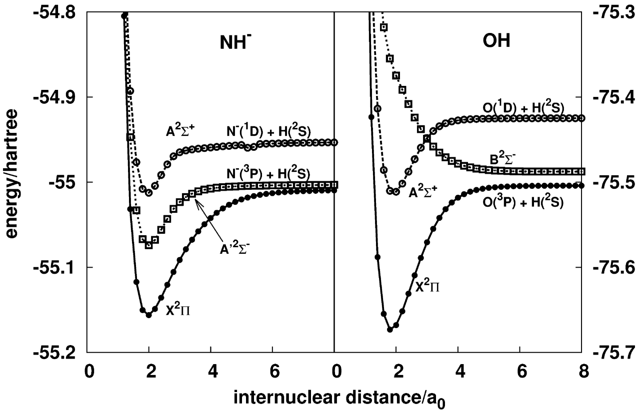

Figure 4. Potential energy curves for the ground state of OH and the ground state of NH^- obtained at the MRCI/CBS level of theory and for the excited states at the MRCI/V6Z level of theory. The excited state $B^2\Sigma^-$ of OH is reported at the MRCI/AVQZ level of theory.

$3.0a_0$ and is higher in energy than the $A^2\Sigma^+$ curve near the equilibrium geometry for the ground state of OH.

It is worth comparing the PECs in reduced variables,[42] that is, $V^*(=V/D_e)$ versus $R^*(=R/R_e)$, where D_e is the bond dissociation energy and R_e is the equilibrium bond distance of the diatomic molecule. The PECs in reduced variables for OH and NH^- are generally superimposable on each other except at the "knee" region, as illustrated in Figure 5.

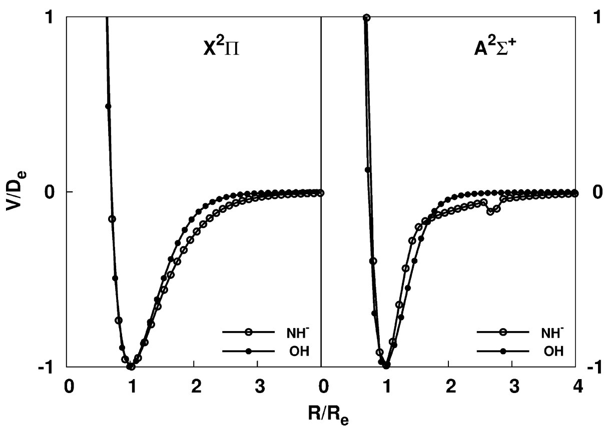

Figure 5. Potential energy curves for the ground and excited states of OH and NH^- in reduced variables.

A similar comparison of other isoelectronic pairs such as (CH^-, NH) and (OH^-, FH) is made and is discussed later.

■ COMPARISON OF OTHER ISOELECTRONIC SPECIES

CH^- and NH. In the case of CH^- and NH, the most important difference is the asymptote of the $A^3\Pi$ state, which corresponds to $C(^3P) + H^-(^1S)$ in CH^- and $N(^2D) + H(^2S)$ in NH, as illustrated in Figure 6. As a result, the $a^1\Delta$ state of CH^- crosses the $A^3\Pi$ state at $5.1a_0$. The PECs for the $A^3\Pi$ and $b^1\Pi$ states of CH^- are nearly superimposable around the equilibrium bond distance but are clearly separated in NH. The plots of PECs in reduced variables are shown in Figure 7 for the ground and excited states of CH^- and NH. The reduced PECs for the $X^3\Sigma^-$ and $a^1\Delta$ states show differences near the "knee" region, whereas the curves for the $A^3\Pi$ state for CH^-

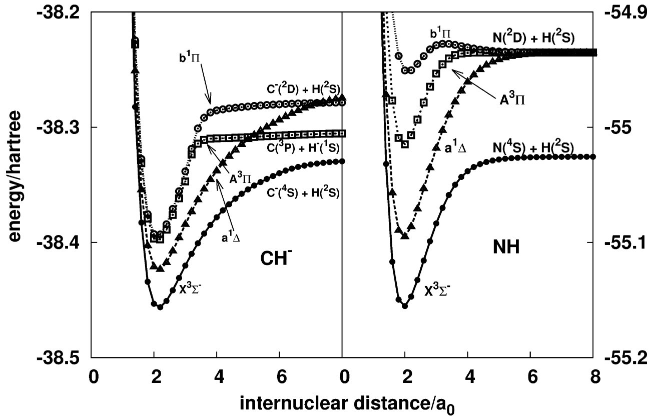

Figure 6. Potential energy curves for the ground state of CH^- obtained at the MRCI/CBS level of theory and for the excited states at the MRCI/AV6Z level of theory. The ground and excited states of NH were obtained at the MRCI/AV5Z level of theory.

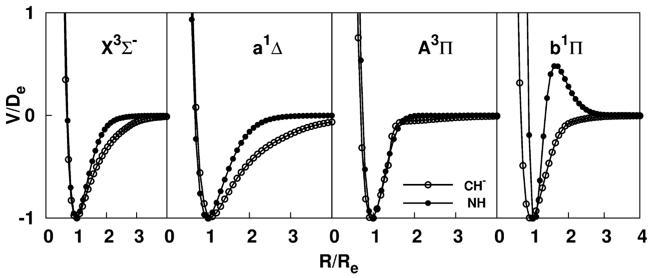

Figure 7. Potential energy curves for the ground state ($X^3\Sigma^-$) and the excited states $a^1\Delta$, $A^3\Pi$, and $b^1\Pi$ of NH and CH^- in reduced variables.

and NH are nearly superimposable. The reduced PEC for the $b^1\Pi$ state of NH shows a big hump, whereas that for CH^- shows a deep well.

OH^- and FH. PECs for the ground state ($X^1\Sigma^+$) and the excited states $a^3\Pi$ and $A^1\Pi$ for OH^- and FH are shown in Figure 8. It can be observed from Figure 8 that both excited states are repulsive for FH and bound for OH^-. The reduced PECs for the ground state of OH^- and FH are nearly superimposable, except in the "knee" region, as illustrated in

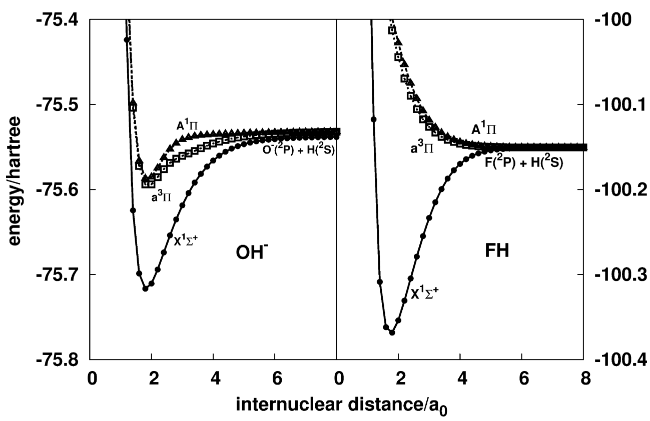

Figure 8. Potential energy curves for the ground state of OH^- obtained at the MRCI/CBS level of theory and for the excited states at the MRCI/V6Z level of theory. The ground and excited states of FH were obtained at the MRCI/AV5Z level of theory.

Figure 9. The PECs for $a^3\Pi$ and $A^1\Pi$ state of NH and OH^- differ considerably.

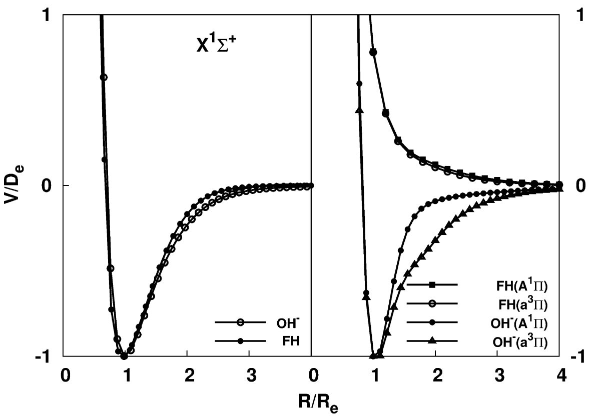

Figure 9. Potential energy curves for the ground and excited states of OH^- and FH in reduced variables.

In summary, a comparison of the PECs for (OH, NH^-), (NH, CH^-), and (OH^-, FH) reveals that the isoelectronic species have comparable PECs in reduced variables for the ground electronic state. Interestingly, the curvature ($k^* = \partial V^*/\partial R^*|_{R^*=1}$) for the neutral species is always larger than that for the isoelectronic anion. For the excited states, the relative ordering of energy levels and their characteristics (repulsive/attractive) differ considerably for the isoelectronic species.

■ CONCLUSIONS

We have computed accurate PECs for the ground ($X^1\Sigma^+$) and excited states ($A^1\Pi$, $a^3\Pi$, and $b^3\Pi$) of OH^- and the ground state ($X^2\Pi$) and the excited state ($A^2\Sigma^+$) of OH. Second moment calculations for the electron distance are used to identify the correct basis set for the ab initio calculation for the resonance states of OH^- buried in the continuum of the OH+e system. Rotational fine structure including Λ-doubling of the ground state of OH has been calculated for the ground and the first excited vibrational states. Using these results, the rotational fine structure of the photodetachment spectrum of OH^- was computed, and it was found to be in good agreement with the experimental results. The lowest threshold value (14 977 cm^{-1}) is proposed as the lower limit of the electron affinity of OH, 237 cm^{-1} larger than the experimental value. We have also discussed the PECs for isoelecronic species in normal variable as well as in reduced variables to show that the order and behavior of the isoelectronic species may not be similar.

■ ASSOCIATED CONTENT

Supporting Information

Plots of second moment calculations. This material is available free of charge via the Internet at http://pubs.acs.org.

■ AUTHOR INFORMATION

Corresponding Author

*E-mail: nsath@iitk.ac.in.

Notes

The authors declare no competing financial interest.

■ ACKNOWLEDGMENTS

We are grateful to Professor Antonio Varandas (Universidade de Coimbra) for initiating us into the investigation of diatomic anions. N.S. is an honorary professor at the Jawaharlal Nehru Center for Advanced Scientific Research, Bangalore. N.S. thanks the Department of Science and Technology, New Delhi for a J C Bose National Fellowship. S.S. thanks the Council of Scientific and Industrial Research, New Delhi for a Senior Research Fellowship.

■ REFERENCES

(1) Branscomb, L. M. Photodetachment Cross Section, Electron Affinity, and Structure of the Negative Hydroxyl Ion. *Phys. Rev.* **1966**, *148*, 11−18.
(2) Cellota, R. J.; Bennett, R. A.; Hall, J. L. Laser Photodetachment Determination of the Electron Affinities of OH, NH_2, NH, SO_2, and S_2. *J. Chem. Phys.* **1974**, *60*, 1740−1745.
(3) Hotop, H.; Patterson, T. A.; Lineberger, W. C. High Resolution Photodetachment Study of OH^- and OD^- in the Threshold Region 7000−6450 Å. *J. Chem. Phys.* **1974**, *60*, 1806−1812.
(4) Owrutsky, J. C.; Rosenbaum, N. H.; Tack, L. M.; Saykally, R. J. The Vibration-Rotation Spectrum of the Hydroxide Anion (OH^-). *J. Chem. Phys.* **1985**, *83*, 5338−5339.
(5) Rosenbaum, N. H.; Owrutsky, J. C.; Tack, L. M.; Saykally, R. J. Velocity Modulation Laser Spectroscopy of Negative Ions: The Infrared Spectrum of Hydroxide (OH^-). *J. Chem. Phys.* **1986**, *84*, 5308−5313.
(6) Goldfarb, F.; Drag, C.; Chaibi, W.; Kröger, S.; Blondel, C.; Delsart, C. Photodetachment Microscopy of the *P*, *Q*, and *R* Branches of the $OH^-(v = 0)$ to OH ($v = 0$) Detachment Threshold. *J. Chem. Phys.* **2005**, *122*, 014308-1−014308-10.
(7) Trippel, S.; Mikosch, J.; Berhane, R.; Otto, R.; Weidemüller, M.; Wester, R. Photodetachment of Cold OH^- in a Multipole Ion Trap. *Phys. Rev. Lett.* **2006**, *97*, 193003-1−193003-4.
(8) Aravind, G.; Gupta, A. K.; Krishnamurthy, M.; Krishnakumar, E. Probing Final-State Interactions in the Photodetachment from OH^-. *Phys. Rev. A* **2007**, *76*, 042714-1−42714-6.
(9) Otto, R.; von Zastrow, A.; Besta, T.; Wester, R. Internal State Thermometry of Cold Trapped Molecular Anions. *Phys. Chem. Chem. Phys.* **2013**, *15*, 612−618.
(10) Cade, P. E. The Electron Affinities of the Diatomic Hydrides CH, NH, SiH and PH. *Proc. Phys. Soc. London* **1967**, *91*, 842−854.
(11) Rosmus, P.; Meyer, W. PNOCI and CEPA Studies of Electron Correlation Effects. VI. Electron Affinities of the First Row and Second Row Diatomic Hydrides and the Spectroscopic Constants of Their Negative Ions. *J. Chem. Phys.* **1978**, *69*, 2745−2751.
(12) Sun, H.; Freed, K. F. Application of Quasidegenerate Manybody Perturbation Theory to the Calculation of Molecular Excited Valence State Negative Ion Feshbach Resonances. *J. Chem. Phys.* **1982**, *76*, 5051−5059.
(13) Werner, H.-J.; Rosmus, P.; Reinsch, E.-A. Molecular Properties from MCSCF-SCEP Wave Functions. I. Accurate Dipole Moment Functions of OH, OH^-, and OH^+. *J. Chem. Phys.* **1983**, *79*, 905−916.
(14) Chipman, D. M. Electron Affinity of Hydroxyl Radical. *J. Chem. Phys.* **1986**, *84*, 1677−1682.
(15) Frenking, G.; Koch, W. A Møller-Plesset Study of the Electron Affinities of the Diatomic Hydrides XH (X = Li,B,Be,C,N,O). *J. Chem. Phys.* **1986**, *84*, 3224−3229.
(16) Lee, T. J.; Schaefer, H. F., III. Systematic Study of Molecular Anions Within the Self-Consistent-Field Approximation: OH^-, CN^-, C_2H^-, NH_2^-, and CH_3^-. *J. Chem. Phys.* **1985**, *83*, 1784−1794.
(17) Ortiz, J. V. Electron Affinity Calculations on NH_2^-, PH_2^-, CN^-, SH^-, OH^-, Cl^-, and F^-: Basis Sets and Direct vs Indirect Methods. *J. Chem. Phys.* **1987**, *86*, 308−312.
(18) Pluta, T.; Sadlej, A. J.; Bartlett, R. J. Polarizability of OH^-. *Chem. Phys. Lett.* **1988**, *143*, 91−96.

(19) Tellinghuisen, J.; Ewig, C. S. Ab Initio Studies of Molecular Anions Stabilized in Point-Charge Lattices: Excited Electronic States of OH^-. *Chem. Phys. Lett.* **1990**, *165*, 355−361.

(20) Sauer, S. P. A.; Møller, C. K.; Koch, H.; Paidarová, I.; Špirko, V. The Vibrational and Temperature Dependence of the Indirect Nuclear Spin-Spin Coupling Constants of the Oxonium (H_3O^+) and Hydroxyl (OH^-) Ions. *Chem. Phys.* **1998**, *238*, 385−399.

(21) Ortiz, J. V. Electron Detachment Energies of Closed-Shell Anions Calculated With A Renormalized Electron Propagator. *Chem. Phys. Lett.* **1998**, *296*, 494−498.

(22) Lefebvre-Brion, H.; Field, R. W. *The Spectra and Dynamics of Diatomic Molecules*; Elsevier Academic: Amsterdam, 2004.

(23) Kayama, K.; Baird, J. C. Spin-Orbit Effects and the Fine Structure in the $^3\sum_g^-$ Ground State of O_2. *J. Chem. Phys.* **1967**, *46*, 2604−2618.

(24) Dunning, T. H., Jr. Gaussian Basis Sets for Use in Correlated Molecular Calculations. I. The Atoms Boron Through Neon and Hydrogen. *J. Chem. Phys.* **1989**, *90*, 1007−1023.

(25) Kendall, R. A.; Dunning, T. H., Jr.; Harrison, R. J. Electron Affinities of the First Row Atoms Revisited. Systematic Basis Sets and Wave Functions. *J. Chem. Phys.* **1992**, *96*, 6796−6806.

(26) Wilson, A. K.; van Mouric, T.; Dunning, T. H., Jr. Gaussian Basis Sets for Use in Correlated Molecular Calculations. VI. Sextuple Zeta Correlation Consistent Basis Sets for Boron Through Neon. *J. Mol. Struct.: THEOCHEM* **1996**, *388*, 339−349.

(27) Werner, H.-J.; Knowles, P. J.; Knizia, G.; Manby, F. R.; Schütz, M.; et al. *Molpro*, A Package of Ab Initio Programs, Version 2010.1. 2010; see http://www.molpro.net.

(28) Varandas, A. J. C. Extrapolating to the One-Electron Basis-Set Limit in Electronic Structure Calculations. *J. Chem. Phys.* **2007**, *126*, 244105-1−244105-15.

(29) Varandas, A. J. C. Extrapolation to the Complete Basis Set Limit Without Counterpoise. The Pair Potential of Helium Revisited. *J. Phys. Chem. A* **2010**, *114*, 8505−8516.

(30) Srivastava, S.; Sathyamurthy, N.; Varandas, A. J. C. An Accurate Ab Initio Potential Energy Curve and the Vibrational Bound States of $X^2\sum_u^-$ State of H_2^-. *Chem. Phys.* **2012**, *398*, 160−167.

(31) Srivastava, S.; Sathyamurthy, N. Radiative Lifetimes of Spin Forbidden $A^1\Delta \rightarrow X^3\sum^-$ and Spin Allowed $A^3\prod \rightarrow X^3\sum^-$ Transitions and Complete Basis Set Extrapolated Ab Initio Potential Energy Curves for the Ground and Excited States of CH^-. *J. Chem. Phys.* **2012**, *137*, 214314-1−214314-8.

(32) Srivastava, S.; Sathyamurthy, N. Ab Initio Potential Energy Curves for the Ground and Low Lying Excited States of NH^- and the Effect of $^2\sum^\pm$ States on L-Doubling of the Ground State $X^2\prod$. *J. Phys. Chem. A* **2013**, *117*, 8623−8631.

(33) LeRoy, R. J. *LEVEL8.0*; University of Waterloo Chemical Physics Research Report No. CP-663; University of Waterloo: Waterloo, Ontario, 2007.

(34) Berning, A.; Schwrizer, M.; Werner, H.-J.; Knowles, P. J.; Palmieri, P. Spin-Orbit Matrix Elements for Internally Contracted Multireference Configuration Interaction Wavefunctions. *Mol. Phys.* **2000**, *98*, 1823−1833.

(35) Parlant, G.; Yarkony, D. R. A theoretical analysis of the state-specific decomposition of OH ($A^2\sum^+, v', N', F_1/F_2$) levels, including the effects of spin-orbit and Coriolis interactions. *J. Chem. Phys.* **1999**, *110*, 363−376.

(36) van der Loo, M. P. J.; Groenenboom, G. C. Theoretical Transition Probabilities for the OH Meinel System. *J. Chem. Phys.* **2007**, *126*, 114314-1−114314-7.

(37) Coxon, J. A.; Foster, S. C. Radial Dependence of Spin-Orbit and Λ-Doubling Parameters in the $X^2\Pi$ Ground State of Hydroxyl. *J. Mol. Spectrosc.* **1982**, *91*, 243−254.

(38) Langhoff, S. R.; Sink, M. L.; Pritchard, R. H.; Kern, C. W. Theoretical Study of the Spin-Orbit Coupling in the $X^2\prod$ State of OH. *J. Mol. Spectrosc.* **1982**, *96*, 200−218.

(39) Mulliken, R. S.; Christy, A. Λ-Type Doubling and Electron Configurations in Diatomic Molecules. *Phys. Rev.* **1931**, *38*, 87−119.

(40) Hinkley, R. K.; Hall, J. A.; Walker, T. E. H.; Richards, W. G. Λ Doubling in $^2\Pi$ States of Diatomic Molecules. *J. Phys. B: At. Mol. Phys.* **1972**, *5*, 204−212.

(41) Blondel, C.; Delsart, C.; Dulieu, F.; Valli, C. Photodetachment Microscopy of O^-. *Eur. Phys. J. D* **1999**, *5*, 207−216.

(42) Abrol, R.; Sathyamurthy, N.; Harbola, M. K. Reduced Potential Energy Curves for Diatomic Molecules and Their Respective Cations. *Chem. Phys. Lett.* **1999**, *312*, 341−345.

(43) Schulz, P. A.; Mead, R. D.; Jones, P. L.; Lineberger, W. C. OH^- and OD^- Threshold Photodetachment. *J. Chem. Phys.* **1982**, *77*, 1153−1165.

(44) Huber, K.; Herzberg, G. *Molecular Spectra and Molecular Structure Vol. 4. Constants of Diatomic Molecules*; Van Nostrand Reinhold: New York, 1979.

(45) Moore, E. A.; Richards, W. G. A Reanalysis of the $A^2\sum^+ - X^2\prod_i$ System of OH. *Phys. Scr.* **1971**, 3, 223−230.

(46) Griffing, K. M.; Simons, J. Theoretical Studies of Molecular Ions. The Ionization Potential and Electron Affinity of BH. *J. Chem. Phys.* **1975**, *62*, 535−540.

(47) Cederbaum, L. S.; Schonhammer, K.; von Niessen, W. Electron Affinities by a Variation-Perturbation Approach. *Phys. Rev. A* **1977**, *15*, 833−842.